Bioconjugate Chemistry

Technical Note

pubs.acs.org/bc

Influence of Nuclides and Chelators on Imaging Using Affibody Molecules: Comparative Evaluation of Recombinant Affibody Molecules Site-Specifically Labeled with ^{68}Ga and ^{111}In via Maleimido Derivatives of DOTA and NODAGA

Mohamed Altai,[†] Joanna Strand,[†] Daniel Rosik,[‡] Ram Kumar Selvaraju,[§] Amelie Eriksson Karlström,[‡] Anna Orlova,[§] and Vladimir Tolmachev*[,†]

[†]Division of Biomedical Radiation Sciences and [§]Preclinical PET Platform, Department of Medicinal Chemistry, Uppsala University, Sweden

[‡]Division of Protein Technology, School of Biotechnology, KTH Royal Institute of Technology, Stockholm, Sweden

ABSTRACT: Accurate detection of cancer-associated molecular abnormalities in tumors could make cancer treatment more personalized. Affibody molecules enable high contrast imaging of tumor-associated protein expression shortly after injection. The use of the generator-produced positron-emitting radionuclide ^{68}Ga should increase sensitivity of HER2 imaging. The chemical nature of radionuclides and chelators influences the biodistribution of Affibody molecules, providing an opportunity to further increase the imaging contrast. The aim of the study was to compare maleimido derivatives of DOTA and NODAGA for site-specific labeling of a recombinant $Z_{HER2:2395}$ HER2-binding Affibody molecule with ^{68}Ga. DOTA and NODAGA were site-specifically conjugated to the $Z_{HER2:2395}$ Affibody molecule having a C-terminal cysteine and labeled with ^{68}Ga and ^{111}In. All labeled conjugates retained specificity to HER2 in vitro. Most of the cell-associated activity was membrane-bound with a minor difference in internalization rate. All variants demonstrated specific targeting of xenografts and a high tumor uptake. The xenografts were clearly visualized using all conjugates. The influence of chelator on the biodistribution and targeting properties was much less pronounced for ^{68}Ga than for ^{111}In. The tumor uptake of ^{68}Ga-NODAGA-$Z_{HER2:2395}$ and ^{68}Ga-DOTA-$Z_{HER2:2395}$ and tumor-to-blood ratios at 2 h p.i. did not differ significantly. However, the tumor-to-liver ratio was significantly higher for ^{68}Ga-NODAGA- $Z_{HER2:2395}$ (8 ± 2 vs 5.0 ± 0.3) offering the advantage of better liver metastases visualization. In conclusion, influence of chelators on biodistribution of Affibody molecules depends on the radionuclides and reoptimization of labeling chemistry is required when a radionuclide label is changed.

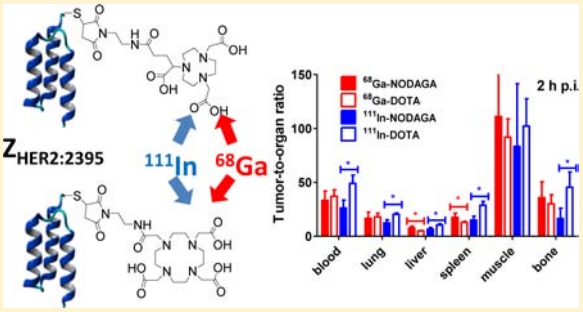

INTRODUCTION

Affibody molecules are small (7 kDa), phage-display derived affinity proteins, which have a substantial potential as imaging agents.[1] They can be selected to bind with high affinity to several cancer-associated molecular abnormalities.[1] The robustness of Affibody molecules permits radiolabeling under harsh conditions. Their small size and high affinity provide good tumor targeting properties and favorable kinetics, thereby permitting acquisition of high contrast images a few hours after injection.[2] The anti-HER2 Affibody molecule $Z_{HER2:342}$ with high affinity (K_D = 22 pM) has been developed previously[3] and is the most studied representative of this class by now. HER2 (human epidermal growth factor receptor type 2) is a transmembrane receptor that is associated with malignant properties in several carcinomas.[4] Signaling of this receptor leads to rapid proliferation, increased motility, and suppression of apoptosis.[4] Targeting of the HER2 with the monoclonal antibody trastuzumab or the tyrosine kinase inhibitor lapatinib is one of the successful approaches to prolong survival of metastatic breast cancer patients.[5] Radionuclide molecular imaging of HER2 expression is a noninvasive approach for selection of patients for HER2-targeted therapy. Preclinical data confirmed the utility of $Z_{HER2:342}$ derivatives in imaging of HER2-expressing tumors.[2] It was found that the HER2-specific Affibody molecule $Z_{HER2:342}$ and its derivatives binds to the binding site (epitope) of HER2 that is different from the binding site of trastuzumab,[6] and saturating concentrations of trastuzumab do not interfere with binding of $Z_{HER2:342}$ derivatives to HER2. This enables the use of radiolabeled $Z_{HER2:342}$ for visualization of changes in HER2 expression induced by therapy utilizing trastuzumab and monitoring response to such therapy.[7] In clinics, radiolabeled Affibody molecules demonstrated the capacity of HER2 imaging in breast cancer metastases.[8,9] Currently, several Affibody molecules for visualization of such cancer-associated molecular

Received: December 20, 2012
Revised: May 21, 2013
Published: May 24, 2013

   dx.doi.org/10.1021/bc300678y | *Bioconjugate Chem.* 2013, 24, 1102−1109

targets as EGFR (epidermal growth factor receptor),[10] IGF1R (insulin-like growth factor 1 receptor),[11] HER3 (human epidermal growth factor receptor type 3),[12] and PDGFRβ (platelet derived growth factor receptor β)[13] are under preclinical evaluation.

The high sensitivity and quantification accuracy of PET would further enhance the utility of Affibody molecules for patient stratification for HER2-targeting therapy and, possibly, for monitoring of response to such therapy. This prompted the labeling of $Z_{HER2:342}$ and its derivatives with positron-emitting radionuclides. Labeling with ^{76}Br,[14] ^{124}I,[15] ^{64}Cu,[16] ^{68}Ga,[17,18] and ^{18}F[7,19,20] provided potential Affibody-based PET imaging agents. Particularly, the generator-produced ^{68}Ga ($T_{1/2}$ = 68 min, E_{β}+max = 1899 keV, 89% β+) is a promising candidate for labeling of Affibody molecules. The rapid kinetics of Affibody molecules are compatible with the short half-life of ^{68}Ga. Potential availability of ^{68}Ge/^{68}Ga generator in clinics might reduce costs and facilitate the production of PET tracers.

Previous data suggest that the labeling chemistry has a profound influence on the tumor targeting properties of Affibody molecules. Small changes in the physicochemical properties of Affibody molecules resulted in modification of the in vivo properties of the tracer, including blood clearance rate, liver uptake, renal retention, and route of excretion.[2] These effects were observed when different chelators and even when the same chelator with different radionuclides were used for labeling of Affibody molecules.[17,21−23] We have shown previously that the use of ^{68}Ga provides higher tumor-to-organ ratios than ^{111}In, when synthetic Affibody molecules were labeled using DOTA conjugated to the N-terminus,[17] or when recombinantly produced Affibody molecules were labeled using maleimido derivatives of NOTA at C-terminus.[19] Recently, we investigated the influence the maleimido derivative of the NODAGA chelator had on the targeting properties of ^{111}In-labeled $Z_{HER2:2395}$ (a variant of anti-HER2 $Z_{HER2:342}$ Affibody molecule having a unique C-terminal cysteine).[23] NODAGA was site-specifically conjugated to $Z_{HER2:2395}$ using a thiol-directed chemistry and labeled with ^{111}In. ^{111}In-NODAGA-$Z_{HER2:2395}$ demonstrated rapid clearance from the blood with lower uptake in normal organs compared to both DOTA- and NOTA-conjugated counterparts.[21,23] Despite the lower tumor uptake observed, the NODAGA-conjugated variant exhibited the highest tumor-to-organ ratios among all three variants. Superiority of ^{68}Ga-labeled NODAGA-conjugated peptides over their DOTA-conjugated analogues has been reported for somatostatin analogues[24,25] and RGD peptides.[26,27] One might expect that the use of maleimido derivative of NODAGA instead of DOTA would also improve the imaging properties of ^{68}Ga-labeled Affibody molecules. This would be essential not only for development of a ^{68}Ga-labeled probe for imaging of HER2 expression in tumors, but also for development of probes for other molecular targets.

We present here a direct comparative in vivo evaluation of a recombinantly produced anti-HER2 $Z_{HER2:2395}$ Affibody molecule containing a C-terminal cysteine and labeled with ^{68}Ga using maleimido derivatives of NODAGA and DOTA (Figure 1) (designated as ^{68}Ga-NODAGA-$Z_{HER2:2395}$ and ^{68}Ga-DOTA-$Z_{HER2:2395}$, respectively). In addition, we have compared the biodistribution of ^{68}Ga-labeled agents in tumor-bearing mice with the biodistribution of their ^{111}In-labeled counterparts.

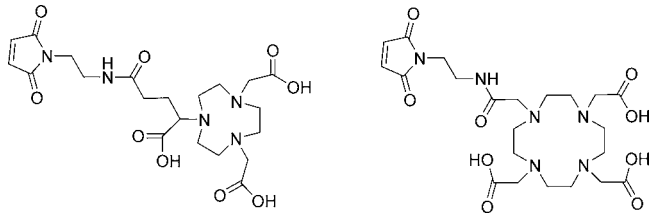

Figure 1. Structure of maleimidomonoamido derivatives of NODAGA (left) and DOTA (right).

MATERIALS AND METHODS

Conjugation and Labeling Chemistry. Maleimidomonoamido derivatives (MMA) of NODAGA and DOTA (Figure 1) were conjugated to $Z_{HER2:2395}$ Affibody molecule having C-terminal cysteine using a site-specific thiol-directed chemistry as described earlier.[23,28] Affinity of the conjugates to HER2 were 67 pM and 74 pM for NODAGA-$Z_{HER2:2395}$ and DOTA-$Z_{HER2:2395}$, respectively.[23] ^{68}Ge/^{68}Ga generator (Eckert and Ziegler) was eluted with 0.1 M hydrochloric acid (prepared from 30% ultrapure HCl from Merck). The generator was pre-eluted 3 h before the labeling. The generator was eluted with 500 μL fractions of 0.1 M HCl. Fraction 3 containing the maximum radioactivity (~60%) was used for labeling.

For labeling with ^{68}Ga, solutions of DOTA-$Z_{HER2:2395}$ and NODAGA-$Z_{HER2:2395}$ (50 μg, 7 nmol) in 60 μL 1.25 M sodium acetate, pH 3.6, were mixed with 167 μL ^{68}Ga-containing eluate (195−270 MBq). The mixture was incubated at 90 °C. Fifteen minutes after start of incubation, a small aliquot (~1 μL) of reaction mixture was taken and analyzed by radio-ITLC (150−771 DARK GREEN, Tec-Control Chromatography strips, Biodex Medical Systems) eluted with 0.2 M citric acid. The ITLC was cross-validated by SDS-PAGE (4−16% bis-tris gel, 200 V constant) as described earlier.[17] The stability of ^{68}Ga-NODAGA-$Z_{HER2:2395}$ and ^{68}Ga-DOTA-$Z_{HER2:2395}$ was evaluated by challenge with 500-fold excess of EDTA as described earlier.[17]

Labeling of NODAGA-$Z_{HER2:2395}$ and DOTA-$Z_{HER2:2395}$ with ^{111}In was performed as described earlier.[23,28]

***In Vitro* Studies.** Specificity of both ^{68}Ga-NODAGA-$Z_{HER2:2395}$ and ^{68}Ga-DOTA-$Z_{HER2:2395}$ binding to HER2-expressing cells was evaluated using ovarian carcinoma SKOV3 (1.6×10^6 receptors/cell)[29] and prostate carcinoma DU-145 (5×10^4 receptors/cell)[30] cell lines purchased from American Type Tissue Culture Collection (ATCC).

An in vitro specificity test was performed according to the methods described earlier.[23] Briefly, a 1 nM solution of ^{68}Ga-NODAGA-$Z_{HER2:2395}$ or ^{68}Ga-DOTA-$Z_{HER2:2395}$ was added to six Petri dishes (ca. 10^6 cells in each). For blocking, a 500-fold excess of nonlabeled recombinant Affibody molecule was added 5 min before the labeled conjugates to saturate the receptors. The cells were incubated during 1 h in a humidified incubator at 37 °C. Thereafter, the media was collected, the cells were detached by trypsin-EDTA solution, and the radioactivity in cells and media was measured to calculate a percentage of cell-bound radioactivity.

A study concerning cellular processing of both conjugates labeled with ^{68}Ga by SKOV3 and DU-145 cells was performed according to the method developed and validated by Wållberg and Orlova.[31] The cells were incubated with 1 nM solution of the labeled compound at 37 °C. At predetermined time points (0.5, 1, 2, and 3 h), cell-bound and internalized radioactivity were determined by an acid wash method. The cells were treated with 0.2 M glycine buffer containing 4 M urea, pH 2.0, for 5 min on

dx.doi.org/10.1021/bc300678y | *Bioconjugate Chem.* 2013, 24, 1102−1109

ice. The radioactivity in the acid fraction was considered as membrane-bound radioactivity. Thereafter, the cells were lysed using 1 M NaOH, and the alkaline fraction was collected. This fraction of radioactivity was considered internalized. The radioactivity of the samples was measured using an automated γ-counter, and data were normalized to the maximum uptake.

***In Vivo* Studies.** The goal of the experiments was a comparative evaluation of the influence of ^{68}Ga and ^{111}In labels on biodistribution and targeting properties of MMA-derivatives of DOTA and NODAGA conjugated to $Z_{HER2:2395}$. All animal experiments were planned and performed in accordance with national legislation on laboratory animals' protection and were approved by the Local Ethics Committee for Animal Research. In order to reduce the number of animals in the experiments, a dual-label approach was used, i.e., ^{68}Ga and ^{111}In-labeled NODAGA-$Z_{HER2:2395}$ were coinjected in the same mice. The same approach was used with the other conjugate DOTA-$Z_{HER2:2395}$. Gamma-spectra of each sample were recorded and uptake of ^{68}Ga and ^{111}In were determined by resolving gamma-spectra as described earlier.[17]

Comparison of tumor targeting was performed in female BALB/c nu/nu mice (15 weeks old, weight 20 ± 1 g) carrying SKOV3 ovarian carcinoma xenografts. Cells (10^7 cells per mouse) were implanted subcutaneously on the right hind leg 3 weeks before the experiment. At the time of injection, the average tumor weight was 100 mg. Eleven mice were injected with a mixture of 10 kBq ^{111}In-NODAGA-$Z_{HER2:2395}$ and 350 kBq ^{68}Ga-NODAGA-$Z_{HER2:2395}$ in 100 μL PBS each. Another group of eleven mice were injected with a mixture of 10 kBq ^{111}In-DOTA-$Z_{HER2:2395}$ and 350 kBq ^{68}Ga-DOTA-$Z_{HER2:2395}$ in 100 μL PBS each. The total amount of injected protein was adjusted to 1 μg (0.14 nmol) per animal by nonlabeled Affibody molecule. At 1 and 2 h postinjection (p.i.), a group of four mice was sacrificed and dissected. The mice were euthanized by an intraperitoneal injection of Ketalar-Rompun solution (20 μL of solution/g body weight: Ketalar, 10 mg/mL; Rompun, 1 mg/mL) followed by heart puncture with a heparinized syringe. Blood and organ samples were collected, weighed, and the radioactivity measured as described above. The organ uptake values were calculated as percent of injected dose per gram of tissue (%ID/g), except for the gastrointestinal tract and the remaining carcass, which were calculated as %ID per whole sample. To check the specificity of xenograft targeting, groups of three mice were subcutaneously preinjected (neck area) with 500 μg (70 nmol) nonlabeled recombinant $Z_{HER2:342}$ Affibody molecule before injecting ^{111}In/^{68}Ga-NODAGA-$Z_{HER2:2395}$ or ^{111}In/^{68}Ga-DOTA-$Z_{HER2:2395}$ mixture. The control groups were sacrificed at 2 h p.i.

Imaging. To confirm the capacity of the conjugates to visualize HER2-expressing tumors an in vivo imaging experiment was performed. For this purpose, four SKOV-3 xenograft bearing mice were separately injected with 1.1 MBq ^{111}In-NODAGA-$Z_{HER2:2395}$ and ^{111}In-DOTA-$Z_{HER2:2395}$ (amount of peptide 1 μg) or with 5 MBq ^{68}Ga-NODAGA-$Z_{HER2:2395}$ and ^{68}Ga-DOTA-$Z_{HER2:2395}$, respectively (amount of peptide 5 μg). Immediately before imaging, the animals were sacrificed and the urine bladders were excised.

All SPECT/CT and PET/CT studies were performed in The Triumph Trimodality system (Gamma Medica, Inc.) a fully integrated SPECT/PET/CT hardware and software platform optimized for small animals in preclinical applications. Images were acquired 1 h p.i. for both the SPECT and PET tracers. SPECT raw data was reconstructed by FLEX SPECT software which uses an ordered Subset Expectation Maximization (OSEM) iterative reconstruction algorithm for its pinhole reconstruction. CT raw files were reconstructed by Filter Back Projection (FBP). SPECT/PET and CT data were fused and analyzed in PMOD (PMOD Technologies Ltd.).

RESULTS

Labeling. Labeling with ^{68}Ga was successful under the selected conditions and the average yield was above 95% (range 96−99%).The SDS-PAGE confirmed the identity and purity of ^{68}Ga-labeled conjugates (Figure 2).

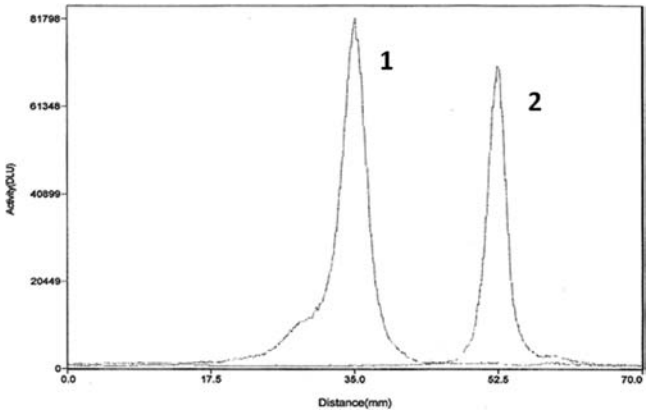

Figure 2. SDS-PAGE analysis of ^{68}Ga-NODAGA-$Z_{HER2:2395}$. Distribution of radioactivity along lanes was visualized and quantified using Cyclone Storage Phosphor System. **1**. ^{68}Ga-NODAGA-$Z_{HER2:2395}$ sample. **2**. ^{68}Ga-acetate sample, which was used as a marker for low molecular weight compounds and free gallium-68.

Stability of ^{68}Ga-NODAGA-$Z_{HER2:2395}$ and ^{68}Ga-DOTA-$Z_{HER2:2395}$ was evaluated by challenge with 500-fold molar excess EDTA at room temperature with subsequent ITLC analysis. The EDTA challenge demonstrated coupling of ^{68}Ga to Affibody molecules was very stable. The radiochemical purity of treated samples was 99.4 ± 0.3%, while the purity of the untreated control was 99.7% for ^{68}Ga-NODAGA-$Z_{HER2:2395}$ and 99% for both treated and untreated ^{68}Ga-DOTA-$Z_{HER2:2395}$, i.e., the difference was within the accuracy of the analytical method.

***In Vitro* Studies.** Binding specificity tests demonstrated that the binding of ^{68}Ga-NODAGA-$Z_{HER2:2395}$ and ^{68}Ga-DOTA-$Z_{HER2:2395}$ to living HER2-expressing cells was receptor-mediated, because presaturation of the receptors by nonlabeled Affibody molecule significantly decreased the binding of the radiolabeled Affibody molecule (for both studied cell lines, $p < 0.0001$) (Table 1). The level of cell-associated radioactivity was appreciably lower for nonblocked DU-145 cell line than for SKOV3 cell line, reflecting the lower expression level of HER2.

Data concerning cellular processing of ^{68}Ga-labeled NODAGA-$Z_{HER2:2395}$ and DOTA-$Z_{HER2:2395}$ are presented in Figure 3. All conjugates demonstrated similar processing pattern typical for $Z_{HER2:342}$ and its derivatives. The internalization rate of both conjugates was slow, but internalized radioactivity was increasing throughout the duration of the study. There were, however, some chelator-related differences in internalized radioactivity. In the case of ^{68}Ga-DOTA-$Z_{HER2:2395}$, 21 ± 4% of radioactivity was internalized at 3 h, while the corresponding value for ^{68}Ga-NODAGA-$Z_{HER2:2395}$ was only 10 ± 3% in the low HER2-expressing DU145 cell line. In contrast, results from the high HER2 expressing SKOV3 cell lines revealed similar internal-

dx.doi.org/10.1021/bc300678y | *Bioconjugate Chem.* 2013, 24, 1102−1109

Table 1. Specificity of Binding of Gallium-68 Labeled Affibody Molecules to HER2-Expressing Cells in Vitro[a]

	Cell-associated radioactivity (% of added)			
	DU-145		SKOV-3	
Conjugate	nonblocked	blocked	nonblocked	blocked
^{68}Ga-NODAGA-Z_{2395}	11.6 ± 0.7	0.09 ± 0.02	48 ± 2	1.2 ± 0.3
^{68}Ga-DOTA-Z_{2395}	11 ± 1	0.4 ± 0.1	41 ± 1	2.8 ± 0.6

[a]The test was performed using the DU-145 prostate cancer and the SKOV-3 ovarian cancer cell lines. For pre-saturation of antigens, a 500-fold molar excess of unlabeled Affibody molecule was added. Data are presented as mean values from three cell dishes with standard deviations.

ization for ^{68}Ga-NODAGA-$Z_{HER2:2395}$ and ^{68}Ga-DOTA-$Z_{HER2:2395}$ (11.0 ± 0.6% vs 9.0 ± 1.6%, respectively).

***In Vivo* Studies.** The data concerning biodistribution of ^{68}Ga and ^{111}In labeled NODAGA-$Z_{HER2:2395}$ and DOTA-$Z_{HER2:2395}$ in female BALB/C nu/nu mice bearing SKOV3 xenografts are presented in Table 2 and Figure 4. All conjugates demonstrated highly specific tumor uptake. Presaturation of HER2 in tumors by preinjection of nonlabeled $Z_{HER2:342}$ caused significant ($p < 0.001$%) reduction of radioactivity accumulation in xenografts for all four conjugates (Figure 4). Preblocking did not cause significant differences in radioactivity concentration in normal organs and tissues (data not shown). The tumor uptake values for ^{68}Ga-DOTA-$Z_{HER2:2395}$, ^{111}In-DOTA-$Z_{HER2:2395}$, and ^{68}Ga-NODAGA-$Z_{HER2:2395}$ were close to each other (no significant difference); the uptake of ^{111}In-NODAGA-$Z_{HER2:2395}$ at both time points was approximately twice lower. All conjugates demonstrated rapid blood clearance and an overall low uptake in nonexcretory organs. The low radioactivity level in the gastrointestinal (GI) tract indicated that the hepatobiliary pathway played a minor role in the excretion of all conjugates. The kidney radioactivity was high for all conjugates indicating predominantly renal excretion with subsequent reabsorption of conjugates in the proximal tubuli.

There were clear chelator and nuclide-dependent differences in the biodistribution pattern of the conjugates. The most pronounced was the difference between ^{111}In-NODAGA-$Z_{HER2:2395}$ and other conjugates. ^{111}In-NODAGA-$Z_{HER2:2395}$ demonstrated significantly more rapid clearance providing significantly lower radioactivity uptake in lung, liver, kidney, gastrointestinal tract, and carcass. The renal accumulation of ^{111}In-NODAGA-$Z_{HER2:2395}$ was more than 2-fold lower in comparison with all other conjugates. The difference between uptake of ^{68}Ga-NODAGA-$Z_{HER2:2395}$ and ^{68}Ga-DOTA-$Z_{HER2:2395}$ at 2 h p.i. was significant only in liver and spleen.

The data concerning tumor-to-organ ratios are presented in Figure 5. ^{68}Ga-NODAGA-$Z_{HER2:2395}$ provided at 2 h after injection significantly higher tumor-to-liver (8 ± 2 vs 5.0 ± 0.4) and tumor-to-spleen (18 ± 4 vs 13 ± 1) ratios than ^{68}Ga-DOTA-$Z_{HER2:2395}$. Remarkably, the difference between ^{111}In-NODAGA-$Z_{HER2:2395}$ and ^{111}In-DOTA-$Z_{HER2:2395}$ was much more pronounced, and ^{111}In-DOTA-$Z_{HER2:2395}$ provided significantly higher tumor-to-blood, tumor-to-lung, tumor-to-liver, tumor-to-spleen, and tumor-to-bone ratios.

Images acquired 1 h after the i.v. injection for the four conjugates into mice bearing SKOV3 xenografts confirmed the capacity of radiolabeled $Z_{HER2:2395}$ derivatives to visualize HER2 expression (Figure 6). In agreement with the biodistribution data, a prominent radioactivity uptake was observed in kidneys.

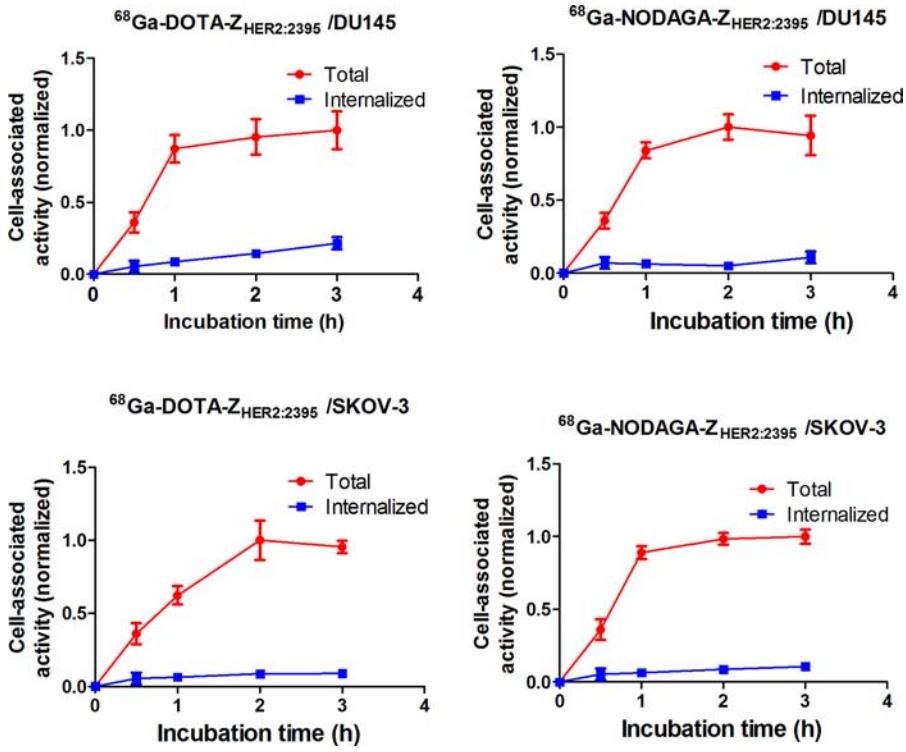

Figure 3. Cell-associated radioactivity as a function of time during continuous incubation of HER2-expressing DU-145 (upper row) and SKOV-3 (lower row) cells with ^{68}Ga labeled Affibody molecules. Data are presented as an average value from 3 dishes ± standard deviation and normalized to the maximum uptake. Error bars might not be seen because they are smaller than the point symbols.

dx.doi.org/10.1021/bc300678y | *Bioconjugate Chem.* 2013, 24, 1102−1109

Table 2. Comparative Biodistribution of NODAGA-$Z_{HER2:2395}$ and DOTA-$Z_{HER2:2395}$ Labeled with Gallium-68 and Indium-111 after Intravenous Injection in Female BALB/C nu/nu Mice Bearing SKOV-3 Xenografts[a]

conjugate	^{68}Ga-NODAGA-$Z_{HER2:2395}$	^{111}In-NODAGA-$Z_{HER2:2395}$	^{68}Ga-DOTA-$Z_{HER2:2395}$	^{111}In-DOTA-$Z_{HER2:2395}$
		Uptake, 1 h pi		
blood	1.8 ± 0.2[c]	1.2 ± 0.2	1.2 ± 0.1[e]	1.2 ± 0.1
lung	2.9 ± 0.2[c]	2.0 ± 0.1	2.1 ± 0.2[e]	2.8 ± 1.2
liver	2.5 ± 0.1[c]	1.52 ± 0.08[f]	3.2 ± 0.4	1.8 ± 0.1[d]
spleen	1.6 ± 0.3[c]	1.0 ± 0.2	1.8 ± 0.3	1.1 ± 0.2[d]
kidney	310 ± 5[c]	122 ± 1[f]	280 ± 19	284 ± 22
tumor	15 ± 8[c]	7.2 ± 3.2[f]	15 ± 2	17 ± 2
muscle	0.4 ± 0.3[c]	0.33 ± 0.04	0.35 ± 0.06	0.37 ± 0.07
bone	1.6 ± 0.3	1.5 ± 0.1[f]	0.8 ± 0.1[e]	0.72 ± 0.09
GI tract[b]	1.4 ± 0.1	1.3 ± 0.3	1.2 ± 0.1	1.6 ± 0.4
carcass[b]	12 ± 3[c]	12 ± 4	8.8 ± 0.4	13 ± 4
		Uptake, 2 h pi		
blood	0.5 ± 0.1	0.3 ± 0.1	0.42 ± 0.07	0.35 ± 0.04
lung	1.0 ± 0.3	0.7 ± 0.1[f]	0.85 ± 0.09	0.84 ± 0.05
liver	2.0 ± 0.3[c]	1.2 ± 0.2[f]	3.1 ± 0.1[e]	1.65 ± 0.05[d]
spleen	0.9 ± 0.1	0.6 ± 0.1	1.2 ± 0.2[e]	0.60 ± 0.03[d]
kidney	297 ± 33[c]	118 ± 13[f]	303 ± 28	313 ± 26
tumor	16 ± 3[c]	8 ± 2[f]	15 ± 1	17 ± 2
muscle	0.14 ± 0.03	0.12 ± 0.09	0.17 ± 0.03	0.18 ± 0.06
bone	0.5 ± 0.1	0.7 ± 0.5	0.6 ± 0.2	0.4 ± 0.1
GI tract[b]	0.7 ± 0.2	0.6 ± 0.1[f]	0.72 ± 0.05	0.8 ± 0.1
carcass[b]	5 ± 1	4.4 ± 0.2[f]	4.6 ± 0.5	6 ± 1[d]

[a]Data are presented as an average % ID/g and standard deviation for four mice. [b]Data for gastrointestinal (GI) tract and carcass are presented as %ID per whole sample. [c]Significant difference ($p < 0.05$) between ^{68}Ga-NODAGA-Z_{2395} and ^{111}In-NODAGA-Z_{2395}. [d]Significant difference ($p < 0.05$) between ^{68}Ga-DOTA-Z_{2395} and ^{111}In-DOTA-Z_{2395}. [e]Significant difference ($p < 0.05$) between ^{68}Ga-NODAGA-Z_{2395} and ^{68}Ga-DOTA-Z_{2395}. [f]Significant difference ($p < 0.05$) between ^{111}In-NODAGA-$Z_{2395}$and ^{111}In-DOTA-Z_{2395}.

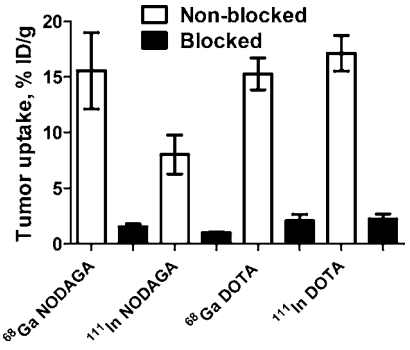

Figure 4. In vivo targeting specificity of ^{68}Ga- and ^{111}In-labeled Affibody molecules in mice bearing SKOV-3 xenografts at 2 h p.i. The blocked group was subcutaneously preinjected with an excess amount of nonlabeled Affibody molecule. Results are presented as percentage of injected activity per gram of tissue (% ID/g).

No noticeable accumulation of radioactivity in other healthy organs and tissues was observed.

DISCUSSION

The use of PET should further increase the sensitivity of imaging using Affibody molecules. This is essential for visualization of small metastases. Emerging production of GMP-grade ^{68}Ga generators suggests that the use of ^{68}Ga as a label might be a way of clinical implementation of Affibody-based PET. Earlier, a number of Affibody variants conjugated with macrocyclic chelators were labeled with ^{111}In and characterized preclinically. These previous studies have demonstrated that both the chemical nature of chelator and conjugation linker, as well as the site of its conjugation to the Affibody molecule, substantially influence the clearance rate of conjugates from blood and their uptake in normal tissues and in tumors.[21−23,32] This opens a way to improve targeting. As much as a 2-fold increase of tumor-to-blood and tumor-to-organ ratios might be gained by optimization of the chelator nature and position in the case of ^{111}In.[21−23,32] One might consider that substitution of ^{111}In with ^{68}Ga in such conjugates could be a straightforward approach requiring only some reoptimization of labeling conditions. However, although both gallium and indium are trivalent metals, they differ appreciably in coordination geometry. In a complex of monoamido derivative of DOTA with gallium, the metal is hexacoordinated and the chelator adopts a *cis*-pseudo-octahedral geometry.[33] Most importantly, one carboxylate group is free and is deprotonated at the physiological pH. Yttrium and indium are octacoordinated, and monoamido derivative of DOTA has somewhat distorted square-antiprismatic geometry having the amide carboxy oxygen involved in chelation.[33] There are no structural data for indium and gallium complexes of NODAGA, but some conclusions might be drawn from information from parental NOTA chelator. NOTA and its derivatives may form trigonal prisms with both indium and gallium, where metals are hexacoordinated.[34] With gallium, both NOTA and its derivative NODASA (1,4,7-triazacyclononane-1-succinic acid-4,7-diacetic acid, a structural analogue of NODAGA) form trigonal prismatic complex, where with N3 and O3 plans almost coplanar.[34,35] Prismatic geometry of indium complexes with NOTA and its

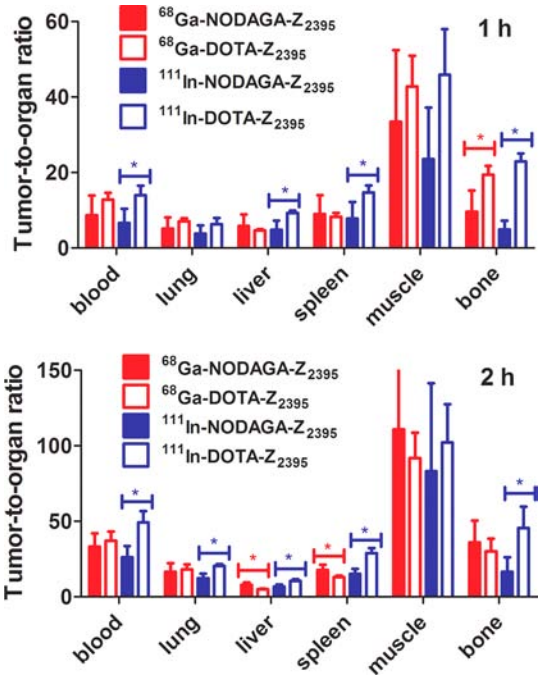

Figure 5. Comparison of tumor-to-organ ratios 1 and 2 h p.i. for ^{68}Ga-DOTA-$Z_{HER2:2395}$ and ^{111}In-DOTA-$Z_{HER2:2395}$, ^{68}Ga-NODAGA-$Z_{HER2:2395}$, and ^{111}In-NODAGA-$Z_{HER2:2395}$ in mice bearing SKOV-3 xenografts. Data are presented as an average and standard deviation for four mice.

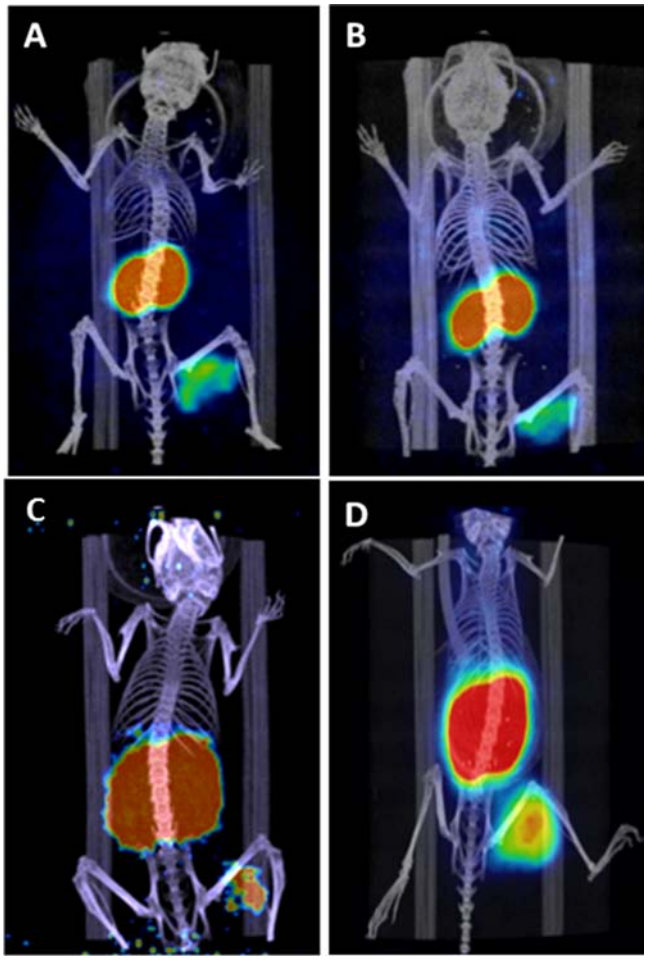

Figure 6. Small-animal SPECT/CT (A and B) and PET/CT (C and D) images (coronal sections) of mice bearing SKOV-3 xenografts at 1 h after injection of ^{111}In-DOTA-$Z_{HER2:2395}$ (A), ^{111}In-NODAGA-$Z_{HER2:2395}$ (B), ^{68}Ga-DOTA-$Z_{HER2:2395}$ (C), and ^{68}Ga-NODAGA-$Z_{HER2:2395}$ (D).

derivatives is appreciably distorted.[36] Moreover, heptacoordinated complexes of indium with NOTA, which include water or chloride, have been reported.[34,37] Structurally different chelates might interfere in different ways with both on-target and off-target interactions of imaging probes and influence their biodistribution. While the difference in biodistribution of ^{111}In and ^{68}Ga-labeled short peptides is quite well studied,[24,38,39] only limited information is available for Affibody molecules.[17,19] In this study, we evaluated Affibody molecules site-specifically coupled at the C-terminus with two different chelators (DOTA and NODAGA) through thiol-directed chemistry. The conjugates are labeled with ^{68}Ga and compared in a dual-label study with ^{111}In.

This study demonstrates that conjugation of maleimido derivatives of DOTA and NODAGA to a unique cysteine at the C-terminus permits site-specific labeling of Affibody molecules with ^{68}Ga and provides high stability of radionuclide attachment. These tracers preserved the capacity to specifically bind HER2-expressing cells in vitro (Table 1). The internalization assay of ^{68}Ga-NODAGA-$Z_{HER2:2395}$ and ^{68}Ga-DOTA-$Z_{HER2:2395}$ showed that internalization rate is slow (Figure 3), which is typical for anti-HER2 Affibody molecules.[17,19,28] Interestingly, the internalization by SKOV-3 cells (high HER2 expression) had nearly equal rates for both conjugates (11 ± 1% vs 9 ± 2% after 3 h incubation). However, this was not the case in DU145 cells (low HER2 expression), where ^{68}Ga-DOTA-$Z_{HER2:2395}$ demonstrated a 2-fold higher internalized fraction compared to ^{68}Ga-NODAGA-$Z_{HER2:2395}$ (21 ± 4% vs 11 ± 3%, respectively). Earlier, we have found that binding of anti-HER2 Affibody molecules to HER2-receptors on DU145 (but not on SKOV3 cell) in vitro might be influenced by coexpression of the target receptors with EGFR, presumably by heterodimerization.[40] It is possible that binding of ^{68}Ga-DOTA-$Z_{HER2:2395}$ and ^{68}Ga-NODAGA-$Z_{HER2:2395}$ influences the heterodimerization of HER2 and EGFR on DU-145 cells differently, which might explain the difference in internalization rate.

Both ^{68}Ga-DOTA-$Z_{HER2:2395}$ and ^{68}Ga-NODAGA-$Z_{HER2:2395}$ targeted HER2-expressing xenografts in mice specifically (Figure 4) and were capable of visualizing HER2-expressing xenografts with high contrast already at 1 h after injection (Figure 6). However, the tumor-to-organ ratios for both conjugates increased appreciably by 2 h after injection (Figure 5). It would make sense to perform imaging at 2 h in clinical practice to visualize small metastases with higher contrast. The 68-min half-life of ^{68}Ga would permit this. Importantly, the biodistribution properties of ^{68}Ga-NODAGA-$Z_{HER2:2395}$ provided significantly higher tumor-to-liver and tumor-to-spleen ratios in comparison with ^{68}Ga-DOTA-$Z_{HER2:2395}$. Thus, the use of maleimido derivative of NODAGA for labeling of Affibody molecules with ^{68}Ga may improve detection of liver metastases. This is important, as liver is a frequent metastatic site for a number of HER2-expressing cancers, including breast carcinoma.[41]

It has to be noted that the biodistribution pattern of ^{111}In-labeled Affibody molecules was not quite predictive for the biodistribution of ^{68}Ga-labeled counterparts. Uptake of both ^{68}Ga-labeled tracers in liver and spleen was significantly higher than that of ^{111}In-labeled. Further, the uptake of ^{111}In-NODAGA-$Z_{HER2:2395}$ was significantly lower than uptake of ^{111}In-DOTA-$Z_{HER2:2395}$ in the majority of tissues, including tumors and kidneys. These results were concordant with our previous data for targeting of DU145 with low HER2 expression,[23] although the magnitude of the effect was different, presumably due to differences in mouse strain, sex, and HER2-expression level in xenografts. Particularly, previous studies[42] have demonstrated that clearance of Affibody molecules from blood is slower in the case of high HER2 expression in tumors, most likely because tumors act as a depot for reversibly bound conjugates. A substantial influence of a chelator and nuclide combination on biodistribution of imaging probes has been observed previously for short peptides. For example, it has been demonstrated that DOTA-RGD peptides labeled with ^{68}Ga have appreciably higher binding to blood proteins than ^{111}In-DOTA-RGD.[39] This resulted in appreciably slower blood clearance of ^{68}Ga-compound, but higher tumor uptake due to higher bioavailability.[39] ^{68}Ga-NODAGA-RGD has appreciably lower adhesion to blood proteins than ^{68}Ga-DOTA-RGD and more rapid blood clearance, but its tumor uptake is also lower.[27] The aforementioned difference in complex geometry is a possible reason for such differences. We could speculate that the distinct biodistribution pattern of ^{111}In-NODAGA-$Z_{HER2:2395}$ had the same cause, although the binding to blood proteins was so subtle it could not be detected ex vivo. The difference in ^{68}Ga-labeled Affibody molecule uptake was limited to liver and spleen.

Overall, while DOTA-$Z_{HER2:2395}$ provided the best tumor-to-organ ratios for ^{111}In label in the model with high HER2 expression, NODAGA-$Z_{HER2:2395}$ was the best for ^{68}Ga.

Interestingly, an earlier study has shown that for synthetic Affibody molecule labeled via DOTA conjugated to N-terminus using amide bond, ^{68}Ga provides equal liver uptake with ^{111}In.[17] In this study, uptake of ^{68}Ga was twice as high as ^{111}In. This indicates that both the position of a chelator in Affibody molecules and conjugation chemistry might influence the biodistribution profile of the imaging agent. Thus assessment of different combinations of radionuclides and chelators is necessary for optimization of scaffold-protein-based imaging agents. Currently, several Affibody molecules are under development as imaging agents for other cancer-associated molecular targets (e.g., EGFR, IGF-1R, PDGFRβ).[1] Moreover, several other scaffold proteins with similar size are evaluated as probes for radionuclide molecular imaging.[43] Our finding should be useful for the development of such probes.

In conclusion, the results of this study suggest that selection of chelators influences biodistribution and imaging properties of Affibody molecules. The use of maleimido derivative of NODAGA instead of DOTA permits an increase of tumor-to-liver and tumor-to-spleen ratios of ^{68}Ga-labeled Affibody molecules in the case of placement of the label at C-terminus. This can be essential for PET visualization of, e.g., small liver metastases. The influence of chelators depends of radionuclides used as labels. Thus, biodistribution data obtained for a scaffold protein conjugate using one nuclide cannot be used for exact prediction of behavior of the same conjugate labeled with another one. This is essential information for the development of imaging conjugates based on scaffold proteins.

AUTHOR INFORMATION

Corresponding Author

*Phone: +46 18 471 3414. Fax: +46 18 471 3432. E-mail: vladimir.tolmachev@bms.uu.se.

Author Contributions

Mohamed Altai and Joanna Strand contributed equally to this study.

Notes

The authors declare no competing financial interest.

ACKNOWLEDGMENTS

This work was financially supported by the Swedish Cancer Society (Cancerfonden) and the Swedish Research Council (Vetenskapsrådet).

REFERENCES

(1) Löfblom, J., Feldwisch, J., Tolmachev, V., Carlsson, J., Ståhl, S., and Frejd, F. Y. (2010) Affibody molecules: engineered proteins for therapeutic, diagnostic and biotechnological applications. *FEBS Lett. 584*, 2670−80.

(2) Ahlgren, S., and Tolmachev, V. (2010) Radionuclide molecular imaging using Affibody molecules. *Curr. Pharm. Biotechnol. 11*, 581−9.

(3) Orlova, A., Magnusson, M., Eriksson, T. L., Nilsson, M., Larsson, B., Höidén-Guthenberg, I., Widström, C., Carlsson, J., Tolmachev, V., Ståhl, S., and Nilsson, F. Y. (2006) Tumor imaging using a picomolar affinity HER2 binding affibody molecule. *Cancer Res. 66*, 4339−48.

(4) Yarden, Y. (2001) Biology of HER2 and its importance in breast cancer. *Oncology 61* (Suppl 2), 1−13.

(5) Arteaga, C. L., Sliwkowski, M. X., Osborne, C. K., Perez, E. A., Puglisi, F., and Gianni, L. (2012) Treatment of HER2-positive breast cancer: current status and future perspectives. *Nat. Rev. Clin. Oncol. 9*, 16−32.

(6) Eigenbrot, C., Ultsch, M., Dubnovitsky, A., Abrahmsén, L., and Härd, T. (2010) Structural basis for high-affinity HER2 receptor binding by an engineered protein. *Proc. Natl. Acad. Sci. U. S. A. 107*, 15039−44.

(7) Kramer-Marek, G., Gijsen, M., Kiesewetter, D. O., Bennett, R., Roxanis, I., Zielinski, R., Kong, A., and Capalam, J. (2012) Potential of PET to predict the response to trastuzumab treatment in an ErbB2-positive human xenograft tumor model. *J. Nucl. Med. 53*, 629−37.

(8) Baum, R. P., Prasad, V., Müller, D., Schuchardt, C., Orlova, A., Wennborg, A., Tolmachev, V., and Feldwisch, J. (2010) Molecular imaging of HER2-expressing malignant tumors in breast cancer patients using synthetic ^{111}In- or ^{68}Ga-labeled affibody molecules. *J. Nucl. Med. 51*, 892−7.

(9) Sandberg, D., Wennborg, A., Feldwisch, F., Tolmachev, V., Carlsson, J., Garske, U., Sörensen, J., and Lindman, H. (2012) First clinical observations of HER2 specific [^{111}In]ABY-025 metastatic detection capability in females with metastatic breast cancer. *J. Nucl. Med. 53* (Supplement 1), 220.

(10) Tolmachev, V., Rosik, D., Wållberg, H., Sjöberg, A., Sandström, M., Hansson, M., Wennborg, A., and Orlova, A. (2010) Imaging of EGFR expression in murine xenografts using site-specifically labelled anti-EGFR ^{111}In-DOTA-$Z_{EGFR:2377}$ Affibody molecule: aspect of the injected tracer amount. *Eur. J. Nucl. Med. Mol. Imaging 37*, 613−22.

(11) Tolmachev, V., Malmberg, J., Hofstrom, C., Abrahmsén, L., Bergman, T., Sjöberg, A., Sandström, M., Gräslund, T., and Orlova, A. (2012) Imaging of insulinlike growth factor type 1 receptor in prostate cancer xenografts using the affibody molecule ^{111}In-DOTA-$Z_{IGF1R:4551}$. *J. Nucl. Med. 53*, 90−7.

(12) Kronqvist, N., Malm, M., Gostring, L., Gunneriusson, E., Nilsson, M., Hoiden Guthenberg, I., Gedda, L., Frejd, F. Y., Ståhl, S., and Löfblom, J. (2011) Combining phage and staphylococcal surface display for generation of ErbB3-specific Affibody molecules. *Protein Eng., Des. Sel. 24*, 385−96.

(13) Lindborg, M., Cortez, E., Hoiden-Guthenberg, I., Gunneriusson, E., von Hage, E., Syud, F., Morrison, M., Abrahmsén, L., Herne, N., Pietras, K., and Frejd, F. Y. (2011) Engineered high-affinity affibody molecules targeting platelet-derived growth factor receptor beta in vivo. *J. Mol. Biol. 407*, 298−315.

(14) Mume, E., Orlova, A., Larsson, B., Nilsson, A. S., Nilsson, F. Y., Sjöberg, S., and Tolmachev, V. (2005) Evaluation of ((4-hydroxyphenyl)ethyl)maleimide for site-specific radiobromination of anti-HER2 affibody. *Bioconjugate Chem. 16*, 1547−55.

(15) Orlova, A., Wållberg, H., Stone-Elander, S., and Tolmachev, V. (2009) On the selection of a tracer for PET imaging of HER2-expressing tumors: direct comparison of a ^{124}I-labeled affibody molecule and trastuzumab in a murine xenograft model. *J. Nucl. Med. 50*, 417−25.

(16) Miao, Z., Ren, G., Liu, H., Jiang, L., and Cheng, Z. (2010) Small-animal PET imaging of human epidermal growth factor receptor positive tumor with a ^{64}Cu labeled affibody protein. *Bioconjugate Chem. 21*, 947−54.

(17) Tolmachev, V., Velikyan, I., Sandström, M., and Orlova, A. (2010) A HER2-binding Affibody molecule labelled with ^{68}Ga for PET imaging: direct in vivo comparison with the ^{111}In-labelled analogue. *Eur. J. Nucl. Med. Mol. Imaging 37*, 1356−67.

(18) Kramer-Marek, G., Shenoy, N., Seidel, J., Griffiths, G. L., Choyke, P., and Capala, J. (2011) ^{68}Ga-DOTA-affibody molecule for in vivo assessment of HER2/neu expression with PET. *Eur. J. Nucl. Med. Mol. Imaging 38*, 1967−76.

(19) Heskamp, S., Laverman, P., Rosik, D., Boschetti, F., van der Graaf, W. T., Oyen, W. J., van Laarhoven, H. W., Tolmachev, V., and Boerman, O. C. (2012) Imaging of human epidermal growth factor receptor type 2 expression with ^{18}F-labeled affibody molecule $Z_{HER2:2395}$ in a mouse model for ovarian cancer. *J. Nucl. Med. 53*, 146−53.

(20) Cheng, Z., De Jesus, O. P., Namavari, M., De, A., Levi, J., Webster, J. M., Zhang, R., Lee, B., Syud, F. A., and Gambhir, S. S. (2008) Small-animal PET imaging of human epidermal growth factor receptor type 2 expression with site-specific ^{18}F-labeled protein scaffold molecules. *J. Nucl. Med. 49*, 804−13.

(21) Tolmachev, V., Altai, M., Sandström, M., Perols, A., Karlström, A. E., Boschetti, F., and Orlova, A. (2011) Evaluation of a maleimido derivative of NOTA for site-specific labeling of affibody molecules. *Bioconjugate Chem. 22*, 894−902.

(22) Malmberg, J., Perols, A., Varasteh, Z., Altai, M., Braun, A., Sandström, M., Garske, U., Tolmachev, V., Orlova, A., and Karlström, A. E. (2012) Comparative evaluation of synthetic anti-HER2 Affibody molecules site-specifically labelled with ^{111}In using N-terminal DOTA, NOTA and NODAGA chelators in mice bearing prostate cancer xenografts. *Eur. J. Nucl. Med. Mol. Imaging 39*, 481−92.
(23) Altai, M., Perols, A., Karlström, A. E., Sandström, M., Boschetti, F., Orlova, A., and Tolmachev, V. (2012) Preclinical evaluation of anti-HER2 Affibody molecules site-specifically labeled with ^{111}In using a maleimido derivative of NODAGA. *Nucl. Med. Biol. 39*, 518−29.
(24) Eisenwiener, K. P., Prata, M. I., Buschmann, I., Zhang, H. W., Santos, A. C., Wenger, S., Reubi, J. C., and Mäcke, H. R. (2002) NODAGATOC, a new chelator-coupled somatostatin analogue labeled with [$^{67/68}$Ga] and [^{111}In] for SPECT, PET, and targeted therapeutic applications of somatostatin receptor (hsst2) expressing tumors. *Bioconjugate Chem. 13*, 530−41.
(25) Fani, M., Del Pozzo, L., Abiraj, K., Mansi, R., Tamma, M. L., Cescato, R., Waser, B., Weber, W. A., Reubi, J. C., and Maecke, H. R. (2011) PET of somatostatin receptor-positive tumors using ^{64}Cu- and ^{68}Ga-somatostatin antagonists: the chelate makes the difference. *J. Nucl. Med. 52*, 1110−8.
(26) Dumont, R. A., Deininger, F., Haubner, R., Maecke, H. R., Weber, W. A., and Fani, M. (2011) Novel ^{64}Cu- and ^{68}Ga-labeled RGD conjugates show improved PET imaging of $\alpha(\nu)\beta(3)$ integrin expression and facile radiosynthesis. *J. Nucl. Med. 52*, 1276−84.
(27) Knetsch, P. A., Petrik, M., Griessinger, C. M., Rangger, C., Fani, M., Kesenheimer, C., von Guggenberg, E., Pichler, B. J., Virgolini, I., Decristoforo, C., and Haubner, R. (2011) [^{68}Ga]NODAGA-RGD for imaging $\alpha v\beta 3$ integrin expression. *Eur. J. Nucl. Med. Mol. Imaging 38*, 1303−12.
(28) Ahlgren, S., Orlova, A., Rosik, D., Sandström, M., Sjöberg, A., Baastrup, B., Widmark, O., Fant, G., Feldwisch, J., and Tolmachev, V. (2008) Evaluation of maleimide derivative of DOTA for site-specific labeling of recombinant affibody molecules. *Bioconjugate Chem. 19*, 235−43.
(29) Tolmachev, V., Tran, T. A., Rosik, D., Sjöberg, A., Abrahmsén, L., and Orlova, A. (2012) Tumor targeting using affibody molecules: interplay of affinity, target expression level, and binding site composition. *J. Nucl. Med. 53*, 953−60.
(30) Malmberg, J., Tolmachev, V., and Orlova, A. (2011) Imaging agents for in vivo molecular profiling of disseminated prostate cancer. Cellular processing of ^{111}In-labeled CHX-A″-DTPA-trastuzumab and anti-HER2 ABY-025 Affibody molecule by prostate cancer cell lines. *Exp. Ther. Med. 2*, 523−528.
(31) Wållberg, H., and Orlova, A. (2008) Slow internalization of anti-HER2 synthetic affibody monomer ^{111}In-DOTA-$Z_{HER2:342\text{-}pep2}$: implications for development of labeled tracers. *Cancer Biother. Radiopharm. 23*, 435−42.
(32) Perols, A., Honarvar, H., Strand, J., Selvaraju, R., Orlova, A., Karlström, A. E., and Tolmachev, V. (2012) Influence of DOTA chelator position on biodistribution and targeting properties of ^{111}In-labeled synthetic anti-HER2 affibody molecules. *Bioconjugate Chem. 23*, 1661−70.
(33) Heppeler, A., Froidevaux, S., Mäcke, H. R., Jermann, E., Béhé, M., Powell, P., and Hennig, M. (1999) Radiometal-labelled macrocyclic chelator-derivatised somatostatin analogue with superb tumour-targeting properties and potential for receptor rmediated internal radiotherapy. *Chem.—Eur. J. 5*, 1974−81.
(34) Broan, C. J., Cox, J. P. L., Craig, A. S., Kataky, R., Parker, D., Harrison, A., Randall, A., and Ferguson, G. J. (1991) Structure and solution stability of indium and gallium complexes of 1,4,7-triazacyclononanetriacetate and of yttrium complexes of 1,4,7,10-tetraazacyclododecanetetraacetate and related ligands: kinetically stable complexes for use in imaging and radioimmunotherapy. X-Ray molecular structure of the indium and gallium complexes of 1,4,7-triazacyclononane-1,4,7-triacetic acid. *J. Chem. Soc., Perkin Trans. 2*, 87−99.
(35) André, J. P., Maecke, H. R., Zehnder, M., Macko, L., and Akyel, K. G. (1998) 1,4,7-Triazacyclononane-1-succinic acid-4,7-diacetic acid (NODASA): a new bifunctional chelator for radio gallium-labelling of biomolecules. *Chem. Commun. 1998*, 1301−1302.
(36) Matthews, R. C., Parker, D., Ferguson, G., Kaitner, B., Harisson, A., and Royle, L. (1991) Synthesis and structure of stable indium and gallium complexes of (R)-1,4,7-tris(2′-methylcarboxymethyl)-triazacyclononane. *Polyhedron 10*, 1951−1953.
(37) Craig, A. S., Helps, I. M., Parker, D., Adams, H., Bailey, N. A., Williams, M. G., Smith, J. M. A., and Ferguson, G. (1989) Crystal and molecular structure of a seven-coordinate chloroindium(III) complex of 1,4,7-triazacyclononanetriacetic acid. *Polyhedron 8*, 2481−2484.
(38) Ginj, M., Zhang, H., Eisenwiener, K. P., Wild, D., Schulz, S., Rink, H., Cescato, R., Reubi, J. C., and Maecke, H. R. (2008) New pansomatostatin ligands and their chelated versions: affinity profile, agonist activity, internalization, and tumor targeting. *Clin. Cancer Res. 14*, 2019−27.
(39) Decristoforo, C., Hernandez Gonzalez, I., Carlsen, J., Rupprich, M., Huisman, M., Virgolini, I., Wester, H. J., and Haubner, R. (2008) ^{68}Ga- and ^{111}In labelled DOTA-RGD peptides for imaging of alphavbeta3 integrin expression. *Eur. J. Nucl. Med. Mol. Imaging 35*, 1507−15.
(40) Barta, P., Malmberg, J., Melicharova, L., Strandgård, J., Orlova, A., Tolmachev, V., Laznicek, M., and Andersson, K. (2012) Protein interactions with HER-family receptors can have different characteristics depending on the hosting cell line. *Int. J. Oncol. 40*, 1677−82.
(41) Disibio, G., and French, S. W. (2008) Metastatic patterns of cancers: results from a large autopsy study. *Arch. Pathol. Lab. Med. 132*, 931−9.
(42) Tolmachev, V., Wållberg, H., Sandström, M., Hansson, M., Wennborg, A., and Orlova, A. (2011) Optimal specific radioactivity of anti-HER2 Affibody molecules enables discrimination between xenografts with high and low HER2 expression levels. *Eur. J. Nucl. Med. Mol. Imaging 38*, 531−9.
(43) Miao, Z., Levi, J., and Cheng, Z. (2011) Protein scaffold-based molecular probes for cancer molecular imaging. *Amino Acids 41*, 1037−47.